Chapter 5

Exact solutions for unsteady axisymmetric flow dynamics of atmospheric vortices

5.1 Introduction

Exact solution of the equations of motion which govern the atmospheric vortices like tornadoes, dust devils etc. has always been a challenging task for the scientific community. This is partly due to complex geometries and partly due to the nonlinear equations of the fluid motion. Tornados and dust-devils occur all over the world under different physical conditions. Dust-devils are formed in the atmospheric

The contents of this chapter are published in Dynamics of Atmospheres and Oceans, 83, 111-121, (2018).

boundary layer whereas tornadoes are born in rotating thunderstorm clouds. Exact solutions of vortex model are most suited for conceptual understanding of the mechanism. There are several analytical vortex models available in the literature for tornadoes, dust-devils and some atmospheric vortices (Rankine, 1882; Burgers, 1948; Rott, 1958; Sullivan, 1959; Davies-Jones and Wood, 2006; Trapp and Jones, 1997).

Results from the observations, numerical simulations and laboratory models show that the azimuthal (swirl velocity) component of the velocity vector in the core region of vortices increases from zero to reah the maximum at the vortex core and decreases in the outer region being inversely proportional to the radial distance. The core is the region around the vertical axis, on the periphery of which the azimuthal velocity is maximum. This type of vortex flow was theoretically modelled first by Rankine (1882) (known as Rankine combined-vortex model). The Rankine combined-vortex model is limited because, it modelled only the azimuthal velocity for inviscid steady flow in an axisymmetric cylindrical geometry with radial and axial velocities considered negligible. The azimuthal velocity in the core region linearly increases with radial distance from the vortex centre and attains the maximum velocity at the outer edge of the core and then decreases like potential vortex. Unlike the Rankine (1882) combined-vortex model, Burgers (1948) and Rott (1958) is a sophisticated model. It is an exact solution of Navier-Stokes equations for the steady, axisymmetric and viscous flows. This model possesses inflow radial velocity which solely depends on radial coordinates, axial velocity, which is a linear function of axial coordinate, and azimuthal velocity, which is dependent on the radial coordinate and also on the fluid viscosity.

To model the real tornado and dust-devil type vortices, both the Rankine combined-vortex and the Burgers vortex models have restrictions and vortices are in

the stationary state in both of them. There are a few time dependent analytical models available in the literature (cf. Davies-Jones and Wood, 2006; Trapp and Jones, 1997; Moffatt, 2000; Kolomenkiy and Moffatt, 2012; Oseen, 1911; Onishchenko et al., 2016; Horton et al., 2016). Oseen (1911) discussed azimuthal velocity only. However, Trapp and Jones (1997) described unsteady azimuthal velocity but the other two are steady. Later, Davies-Jones and Wood (2006) validated their model with tornado's motion. Moffatt (2000) and Kolomenkiy and Moffatt (2012) considered all the three unsteady components of vortex motion while investigation different aspects. Moffatt (2000) tried to address the problem of blow up introduced by Leray (1934) and provided a solution to Leray's equation which is a reduced Navier-Stokes equation; while Kolomenkiy and Moffat (2012) reported similarity solutions for unsteady stagnation point flow. Onishchenko et al. (2016) reported a vortex model for dust devils in which all the components are unsteady and grow exponentially.

Burgers (1948) and Rott (1958) model is an axisymmetric vortex solution given by $u = -Ar$, $v = v(r)$, $w = 2Az$ in the cylindrical polar coordinates (r, θ, z), where u, v, w are respectively the radial, the azimuthal and the axial velocities. Wondering over the fact how some simple exact solutions remained unreported despite rigorous exercises carried out for understanding vortex motion, Craik (2009) presented some solutions by different time independent and time dependent assumptions for the radial flow parameters $A(t)$ and $B(t)$ of the corresponding generalised assumed solutions given by $u = A(t)r + B(t)/r$, $w = -2A(t)z$. We have observed that there can be a non-steady more general time dependent exact solutions for $A(t)$ with the assumption that $B = 0$. The various assumptions for $A(t)$ by Davies-Jones and Wood (2006), Moffatt (2000), Kolomenkiy and Moffat (2012) and Craik (2009) will be special cases of this solution. All these results are discussed in the chapter, in detail, whenever and wherever required.

The solutions are presented here.

5.2 Mathematical model

5.2.1 Formulation of the problem

We start the analysis in cylindrical polar coordinates (r, θ, z) for modelling atmospheric vortices, where r, θ, z respectively stand for radial, angular and axial coordinates bounded by the radius $(0 \leq r \leq R)$ and the height $(0 \leq z \leq H)$. We only consider the axisymmetric case so that terms are independent of the angular coordinate θ. Moreover, body forces are neglected. Hence, the equations of motion governing the unsteady axisymmetric flow for dry atmosphere may be given by

$$\frac{\partial u}{\partial t} + u\frac{\partial u}{\partial r} + w\frac{\partial u}{\partial z} - \frac{v^2}{r} = -\frac{1}{\rho}\frac{\partial p}{\partial r} + \nu\left\{\frac{\partial^2 u}{\partial r^2} + \frac{1}{r}\frac{\partial u}{\partial r} - \frac{u}{r^2} + \frac{\partial^2 u}{\partial z^2}\right\}, \tag{5.1}$$

$$\frac{\partial v}{\partial t} + u\frac{\partial v}{\partial r} + w\frac{\partial v}{\partial z} + \frac{uv}{r} = \nu\left\{\frac{\partial^2 v}{\partial r^2} + \frac{1}{r}\frac{\partial v}{\partial r} - \frac{v}{r^2} + \frac{\partial^2 v}{\partial z^2}\right\}, \tag{5.2}$$

$$\frac{\partial w}{\partial t} + u\frac{\partial w}{\partial r} + w\frac{\partial w}{\partial z} = -\frac{1}{\rho}\frac{\partial p}{\partial z} + b + \nu\left\{\frac{\partial^2 w}{\partial r^2} + \frac{1}{r}\frac{\partial w}{\partial r} + \frac{\partial^2 w}{\partial z^2}\right\}, \tag{5.3}$$

$$\frac{1}{r}\frac{\partial (ru)}{\partial r} + \frac{\partial w}{\partial z} = 0. \tag{5.4}$$

where (u, v, w) are the velocity components in the radial (r), the azimuthal (θ) and the axial (z) directions, t is time, ρ is the constant density, p is the pressure and ν is the viscosity.

We consider that the velocity at the lower surface satisfies no-slip condition at the ground level. Following the assumption of Burgers (1948) model, we prescribe the radial and the axial velocity components as given below with the following

generalisation:

$$u(r,t) = -A(t)r,\ w(z,t) = 2A(t)z, \tag{5.5}$$

and intend to formulate the azimuthal component of velocity as a consequence of imposed conditions. Burgers (1948) and Rott (1958) considered A a constant in order to model the swirl velocity for the steady vortex while Davies-Jones and Wood (2006) and Trapp and Jones (1997) considered A as constant and investigated the time dependent extension of Rankine (1882) combined-vortex model for an inviscid fluid and time dependent Burgers (1948) model for viscous vortex flow. Further, Moffatt (2000) as well as Kolomenkiy and Moffatt (2012) made the assumption that $A(t) \propto 1/(t_0 - t)$, where t_0 is constant.

The assumptions made in Eq. (5.5) satisfy the continuity equation (5.4) and, in view of them, Eqs. (5.1)−(5.3) reduce to

$$\frac{\partial p}{\partial r} = \rho\left(\frac{dA(t)}{dt} - A^2(t)\right)r + \rho\frac{v^2(r,t)}{r}, \tag{5.6}$$

$$\frac{\partial v}{\partial t} - A(t)r\left(\frac{\partial v}{\partial r} + \frac{v}{r}\right) + 2A(t)z\frac{\partial v}{\partial z} = \nu\left(\frac{\partial^2 v}{\partial r^2} + \frac{1}{r}\frac{\partial v}{\partial r} - \frac{v}{r^2} + \frac{\partial^2 v}{\partial z^2}\right), \tag{5.7}$$

$$\frac{\partial p}{\partial z} = -2\rho\left(\frac{dA(t)}{dt} + 2A^2(t)\right)z, \tag{5.8}$$

Eq. (5.6) and Eq. (5.8) implies that the azimuthal velocity is independent of the axial coordinates z. In view of this, Eq. (5.7) may be rewritten as

$$\frac{\partial v}{\partial t} = A(t)r\left(\frac{\partial v}{\partial r} + \frac{v}{r}\right) + \nu\left(\frac{\partial^2 v}{\partial r^2} + \frac{1}{r}\frac{\partial v}{\partial r} - \frac{v}{r^2}\right), \tag{5.9}$$

Radial pressure gradient is required to maintain circulation in tornadoes and dust-devils. Researchers used cyclostrophic balance to determine the radial pressure gradients or pressure distributions in these types of vortex flow. There are

analytical solutions of Eq. (5.9) available in the literature with the assumptions that $A(t) = 0$ or constant. But we are looking for a more general solution.

5.2.2 Evaluation of A(t)

We shall evaluate $A(t)$ for different cases of axial pressure gradient.

Case 1: In Rankine's combined-vortex model for the steady state flow, the radial and the axial pressure gradients are respectively given by $\partial p/\partial r = \rho v^2/r$, and $\partial p/\partial z = 0$, where $\partial p/\partial r = \rho v^2/r$, represents the cyclostrophic balance in the atmospheric flow.

Under the consideration that $\partial p/\partial z = 0$, Eq. (5.8) reduces to

$$\frac{dA(t)}{dt} + 2A^2(t) = 0, (0 \leq t < t_\infty)$$

which, under the initial condition $A(t_0) = A_0$, gives

$$A(t) = \frac{A_0}{2A_0 \times (t - t_0) + 1}, \tag{5.10}$$

Case 2: In the steady Burgers (1948) and Rott (1958) vortex model, the radial and the axial pressure gradients are respectively given by

$$\frac{\partial p}{\partial r} = -\rho a^2 r + \rho \frac{v^2}{r}, \quad \frac{\partial p}{\partial z} = -4\rho a^2 z,$$

where a is a constant.

Substituting the axial pressure gradient of this case in Eq. (5.8), we get

$$\frac{dA(t)}{dt} + 2A^2(t) - 2a^2 = 0,$$

which yields

$$A(t) = \frac{a\,(1 + Le^{-4at})}{(1 - Le^{-4at})},$$

where L is evaluated for $t = t_0$ under the condition that $A(t_0) = A_0$ to get, $L = (A_0 - a)/(A_0 + a)$,

Hence

$$A(t) = \frac{a\left\{1 + \frac{(A_0-a)}{(A_0+a)}e^{-4a(t-t_0)}\right\}}{1 + \frac{(A_0-a)}{(A_0+a)}e^{-4a(t-t_0)}}. \tag{5.11}$$

which reduces to A_0 of the Burgers model as $t \to t_0$.

5.2.3 Determination of azimuthal velocity for inviscid flows

Now we solve Eq. (5.9) for inviscid flow. In terms of angular momentum $M(r,t) = rv(r,t)$, Eq. (5.9) reduces to the Lagrange's linear form given by

$$\frac{\partial M(r,t)}{\partial t} - A(t)r\frac{\partial M(r,t)}{\partial r} = 0, \tag{5.12}$$

Using the method of characteristic along with the assumption that the angular momentum is constant along the characteristic, Eq. (5.12) has the following characteristic curve:

$$r(t) = r(t_0)e^{-\int_{t_0}^{t} A(s)ds},$$

where $r(t_0)$ is the initial inner radius of the vortex. Since there is no diffusion, the core wall of the vortex advects the flow. The core radius may be given by

$$\delta(t) = \delta(t_0)e^{-\int_{t_0}^{t} A(s)ds}, \tag{5.13}$$

where $\delta(t_0)$ is the initial core radius. Following the Rankine combined-vortex model, the unsteady azimuthal velocity may be considered as

$$v(r,t) = \begin{cases} v_m(t) r/\delta(t), \ for\ r \leq \delta(t) \\ v_m(t)\delta(t)/r, \ for\ r > \delta(t) \end{cases}, \tag{5.14}$$

For $t = 0$, this azimuthal velocity reduces to the azimuthal velocity for the steady Rankine (1882) combined vortex model. Here $v_m(t)$ is the maximum azimuthal velocity at time t and $\delta(t)$ is the core radius, where the fluid attains the maximum azimuthal velocity. The angular momentum is constant along the core wall and also in the outer region of the core. This implies that the circulation is constant. Therefore, the maximum azimuthal velocity $v_m(t)$ at any instant is given by

$$v_m(t) = \frac{M_\infty}{\delta(t)} = \frac{M_\infty}{\delta(t_0)} e^{\int_{t_0}^{t} A(s)ds} = \frac{M_\infty}{\delta(t_0)\sqrt{2 \times A_0(t-t_0)+1}}. \tag{5.15}$$

Thus, Eq. (5.14) reduces to

$$v(r,t) = \begin{cases} \frac{M_\infty}{\delta^2(t)} r, \ for\ r \leq \delta(t) \\ \frac{M_\infty}{r}, \ for\ r > \delta(t) \end{cases}, \tag{5.16}$$

Substituting Eq. (5.13) into Eq. (5.16), the azimuthal velocity for an unsteady vortex may be given by

$$v(r,t) = \begin{cases} \frac{M_\infty}{\delta^2(t_0)} e^{2\int_{t_0}^{t} A(s)ds}, \ for\ r \leq \delta(t) \\ \frac{M_\infty}{r}, \ for\ r > \delta(t) \end{cases}, \tag{5.17}$$

Eq. (5.5) and Eq. (5.17) represent an unsteady combined vortex model. For constant A, this reduces to the inviscid flow solution reported by Davies-Jones and Wood

(2006) and Trapp and Jones (1997).

In subsection (5.2.2), we have obtained two different expressions of $A(t)$ for two different cases. We use the two to get the following expressions of core radius and angular velocity:

Substituting $A(t)$ from Eq. (5.10) into Eq. (5.13), the core radius $\delta(t)$, obtained for the unsteady combined-vortex model, is given by

$$\delta(t) = \frac{\delta(t_0)}{\sqrt{2 \times A_0(t - t_0) + 1}}, \tag{5.18}$$

which reduces to $\delta(t_0)$ of the Rankine (1882) combined-vortex as $t \to t_0$. We further observe that $\delta(t) \to 0$ when $t \to \infty$. Corresponding azimuthal angular velocity of the core region for inviscid motion with zero axial pressure gradient is

$$\omega(t) = \frac{M_\infty}{\delta^2(t_0)} \left\{2 \times A_0(t - t_0) + 1\right\}. \tag{5.19}$$

The angular velocity $\omega(t)$ becomes constant as in the Rankine (1882) combined-vortex when $t \to t_0$.

Further, substituting $A(t)$ from Eq. (5.11) into Eq. (5.13), the same is obtained as

$$\delta(t) = \delta(t_0)\sqrt{\frac{2a}{A_0 \sinh 2a(t - t_0) + a \cosh 2a(t - t_0)}}. \tag{5.20}$$

Here too, $\delta(t) \to \delta(t_0)$ as $t \to t_0$; and $\delta(t) \to 0$ when $t \to \infty$.

Corresponding angular velocity of the core region for inviscid motion with non-zero axial pressure gradient is

$$\omega(t) = \frac{M_\infty}{\delta^2(t_0)} \left\{\frac{A_0 \sinh 2a(t - t_0) + a \cosh 2a(t - t_0)}{2a}\right\} \tag{5.21}$$

5.2.4 Determination of azimuthal velocity for viscous flows

For viscous flow in terms of angular momentum, which is $M(r,t) = rv(r,t)$, Eq. (5.9) reduces to

$$\frac{\partial M(r,t)}{\partial t} - A(t)r\frac{\partial M(r,t)}{\partial r} = \nu r\frac{\partial}{\partial r}\left(\frac{1}{r}\frac{\partial M(r,t)}{\partial r}\right). \tag{5.22}$$

We solve Eq. (5.22) for the swirling flow, i.e., for the vortex having finite non-zero circulation $\Gamma_\infty = 2\pi M_\infty$ at infinity. Similarity solution of Eq. (5.22) is obtained from the consideration that $M(r,t) = rv(r,t) = M(\zeta)$, where $\zeta = r/\delta(t)$. In view of this, Eq. (5.22) transforms to

$$\frac{d^2M(\zeta)}{d\zeta^2} + \left\{\frac{1}{\nu}\left(\delta(t)\frac{d\delta(t)}{dt} + A(t)\delta^2(t)\right)\zeta - \frac{1}{\zeta}\right\}\frac{dM(\zeta)}{d\zeta} = 0,$$

which may be rewritten as

$$\delta(t)\frac{d\delta(t)}{dt} + A(t)\delta^2(t) = \frac{\nu}{\zeta}\left[\frac{\frac{d^2M(\zeta)}{d\zeta^2}}{\frac{dM(\zeta)}{d\zeta}} + \frac{1}{\zeta}\right] = \nu C\ (say), \tag{5.23}$$

where C is a constant, since on the left side is a function of only t and on the other is a function of only ζ.

The second equality of Eq. (5.23) may be manipulated as

$$\frac{d^2M(\zeta)}{d\zeta^2} + \left(C\zeta - \frac{1}{\zeta}\right)\frac{dM(\zeta)}{d\zeta} = 0. \tag{5.24}$$

Solving this, we get

$$\frac{dM(\zeta)}{d\zeta} = C_1\zeta\exp\left(-C\frac{\zeta^2}{2}\right),$$

which further gives

$$M(\zeta) - M(\zeta_0) = C_1 \int_{\zeta_0}^{\zeta} \zeta^{'} \exp\left(-C\frac{\zeta^{'2}}{2}\right) d\zeta^{'},$$

i.e.

$$M(\zeta) = M(\zeta_0) + \frac{\nu C_1}{C} e^{-C\zeta_0^2/2}\left[1 - e^{-C\left(\zeta^2-\zeta_0^2\right)/2}\right].$$

Since r_0, C and $\delta(t_0)$ are fixed, we assume $\frac{\nu C_1}{C} e^{-C\zeta_0^2/2} = K$, and K is to be determined by using the condition that the circulation $\Gamma = 2\pi M(\zeta)$ is finite (say M_∞) and non-zero when $r \to \infty (\zeta \to \infty)$. Thus, the above equation gives

$$M(\zeta) = M(\zeta_0) + (M_\infty - M(\zeta_0))\left[1 - e^{-C\left(\zeta^2-\zeta_0^2\right)/2}\right] \tag{5.25}$$

When $M(\zeta_0) = 0$ for $\zeta_0 = 0$, the above relation reduces the same expression investigated by Davies-Jones and Wood (2006) and Trapp and Jones (1997).
In order to determine $\delta(t)$, we rearrange Eq. (5.23) as

$$\frac{d\delta^2(t)}{dt} + 2A(t)\delta^2(t) = 2\nu C, \text{ or } \frac{d\delta(t)}{dt} + A(t)\delta(t) = \frac{\nu C}{\delta(t)}.$$

This equation gives the velocity of the core wall. Integrating this, we obtain the core radius $\delta(t)$ as

$$\delta^2(t) = \delta^2(t_0)\exp\left(-2\int_{t_0}^{t} A(s)ds\right) + 2\nu C \exp\left(-2\int_{0}^{t} A(s)ds\right)\int_{t_0}^{t}\exp\left(2\int_{0}^{s} A(s_1)ds_1\right)ds,$$

which reduces to

$$\delta^2(t) = \delta^2(t_0)\exp\left\{-2A \times (t - t_0)\right\} + \frac{\nu C}{A}\left[1 - \exp\left\{-2A \times (t - t_0)\right\}\right],$$

for A being a constant. This is the expression for the core radius reported by Davies-Jones and Wood (2006) and Trapp and Jones (1997), where C is constant and is determined by using the assumption that the maximum azimuthal velocity occurs at the core radius $r = \delta(t)$.

For the two cases of pressure gradient, having different values of $A(t)$, discussed in Subsection (5.2.2), the core radius is given respectively by

$$\delta^2(t) = \frac{\delta^2(t_0)}{2(t-t_0)A_0 + 1} + \frac{2(t-t_0)\nu C}{2(t-t_0)A_0 + 1}\left\{(t-t_0)A_0 + 1\right\}. \tag{5.26}$$

For $\nu \to 0$, Eq. (5.26) reduces to Eq. (5.18) meant for inviscid flow. Unlike inviscid case, $\delta(t) \to \infty$ when $t \to \infty$ for viscous flows due to the presence of the second term involving viscosity on the right side of the equation.

$$\begin{aligned}\delta^2(t) = \delta^2(t_0)\left\{\frac{a}{A_0 \times \sinh 2a(t-t_0) + a \times \cosh 2a(t-t_0)}\right\} \\ + \frac{\nu C}{a}\left\{\frac{A_0 \times \{\cosh 2a(t-t_0) - 1\} + a \times \sinh 2a(t-t_0)}{A_0 \times \sinh 2a(t-t_0) + a \times \cosh 2a(t-t_0)}\right\}.\end{aligned} \tag{5.27}$$

It is observed from Eq. (5.26) and Eq. (5.27) both that $\delta(t) \to 1$ as $t \to t_0$. However, in Eq. (5.26), $\delta(t) \to \infty$ as $t \to \infty$ but in Eq. (5.27),

$$\delta(t) \to \begin{cases} \sqrt{\nu C/a}\ as\ t \to \infty\ (provided\ a \neq 0) \\ \infty,\ as\ t \to \infty\ (when\ a \to 0) \end{cases},$$

This is to be noted that the inference $\delta(t) \to \infty$ when $a \to 0$, is similar to the conclusion made for the previous case of zero axial pressure gradient formulated in Eq. (5.26).

Using equations Eq. (5.26) and Eq. (5.27), the unsteady azimuthal velocity in terms of angular momentum is given by

$$M(r,t) = M(\zeta_0) + (M_\infty - M(\zeta_0)) \left[1 - \exp\left\{-\frac{C}{2}\left(\frac{r^2}{\delta^2(t)} - \frac{r_0^2}{\delta^2(t_0)}\right)\right\}\right]. \quad (5.28)$$

Corresponding azimuthal velocity is given by

$$v(r,t) = \frac{M(\zeta_0)}{r} + \frac{(M_\infty - M(\zeta_0))}{r} \left[1 - \exp\left\{-\frac{C}{2}\left(\frac{r^2}{\delta^2(t)} - \frac{r_0^2}{\delta^2(t_0)}\right)\right\}\right]. \quad (5.29)$$

Eq. (5.29) together with Eq. (5.5), in which $A(t)$ is given by either Eq. (5.10) or Eq. (5.11), represents an unsteady model, which reduces to the corresponding steady state Burgers (1948) and Rott (1958) model for constant A.

When the initial angular momentum of the wind in the atmospheric vortex is zero i.e. $M(\zeta_0) = 0$ when $r = r_0 = 0$ and A is constant, then Eq. (5.29) reduces to the azimuthal velocity given by Trapp and Jones (1997) and Davies-Jones and Wood (2006). We have $M(\zeta_0) = 0$ for $\zeta_0 = 0$, which is achieved when $r_0 = 0$. The unsteady azimuthal velocity for a one-celled vortex given by Bellamy-Knights (1970) is a special case of Eq. (5.29) with their assumption, i.e. $A(t) \propto 1/t$. Further, Eq. (5.29) reduces to the azimuthal velocity given by Moffatt (2000) and, Kolomenkiy and Moffatt (2012) for the assumption that $A(t) \propto 1/(t_0 - t)$, where t_0 is constant.

We determine C in the following way: The maximum azimuthal velocity occurs at $r = \delta(t)$ and therefore

$$\frac{\partial p}{\partial r} = 0, \ \frac{\partial^2 v}{\partial r^2} < 0, \ at \ r = \delta(t). \quad (5.30)$$

Using this condition in Eq. (5.29), we get

$$1+\frac{C}{\nu}=\left(1+\frac{M(\zeta_0)}{M(\zeta_0)-M_\infty}\right)\exp\left\{\frac{C}{2}\left(1-\frac{r_0^2}{\delta^2(t_0)}\right)\right\}. \tag{5.31}$$

This can be solved to evaluate C.

Substituting $r=\delta(t)$ in Eq. (5.29) and the value of C obtained from Eq. (5.31), we can have the maximum tangential velocity at any instant from

$$v_m(t)=\frac{M(\zeta_0)}{\delta(t)}+\frac{(M_\infty-M(\zeta_0))}{\delta(t)}\left[1-\exp\left\{-\frac{C}{2}\left(1-\frac{r_0^2}{\delta^2(t_0)}\right)\right\}\right]. \tag{5.32}$$

For $M(\zeta_0)=0$ as $r_0=0$, Eq. (5.31) reduces to

$$1+C=\exp\left(\frac{C}{2}\right),$$

which gives $C=2.5128$. Thus, the maximum tangential velocity for this case is given by

$$v_m(t)=\frac{M_\infty}{\delta(t)}\left[1-\exp\left(-1.2564\right)\right]=\frac{0.71532\times M_\infty}{\delta(t)}. \tag{5.33}$$

Eq. (5.33) is similar to the expression derived by Davies-Jones and Wood (2006) for the core radius for constant A.

Substituting $A(t)$ from Eq. (5.10) and Eq. (5.11) into Eq. (5.6), we get the radial pressure for the two cases of $A(t)$,

$$\frac{\partial p}{\partial r}=-\frac{3\rho A_0^2 r}{\{2(t-t_0)A_0+1\}^2}+\frac{\rho}{r^3}\left[M_\infty+(M(\zeta_0)-M_\infty)\exp\left\{-\frac{C}{2}\left(\frac{r^2}{\delta^2(t)}-\frac{r_0^2}{\delta^2(t_0)}\right)\right\}\right]^2. \tag{5.34}$$

for which $\delta^2(t)$ is given by Eq. (5.26).

$$\frac{\partial p}{\partial r} = -\frac{\rho a^2 \left\{1 + 10\left(\frac{A_0-a}{A_0+a}\right)e^{-4a(t-t_0)} + \left(\frac{A_0-a}{A_0+a}\right)^2 e^{-8a(t-t_0)}\right\}}{\left\{1 - \left(\frac{A_0-a}{A_0+a}\right)e^{-4a(t-t_0)}\right\}^2} + \frac{\rho}{r^3}\left[M_\infty + (M(\zeta_0) - M_\infty)\exp\left\{-\frac{C}{2}\left(\frac{r^2}{\delta^2(t)} - \frac{r_0^2}{\delta^2(t_0)}\right)\right\}\right]^2. \tag{5.35}$$

for which $\delta^2(t)$ is given by Eq. (5.27).

Eurther, in view of Eq. (5.29) the axial vorticity for viscous motion is given by

$$\Omega_z(r,t) = \frac{1}{r}\frac{\partial\left(rv(r,t)\right)}{\partial r} = \frac{C\left(M_\infty - M(\zeta_0)\right)}{\delta^2(t)}\exp\left\{-\frac{C}{2}\left(\frac{r^2}{\delta^2(t)} - \frac{r_0^2}{\delta^2(t_0)}\right)\right\}. \tag{5.36}$$

5.3 Results and discussion

Our generalised equations for the various cases are used to plot graphs exhibiting influence of various parameters on various entities characterising the unsteady flows.

We plot graphs for core radius $\delta(t)$ against time t. For $\delta(t)$, we have two forms related to two different cases: one for inviscid flows and the other for viscous flows. Both have been further categorised into two parts depending on the value of $A(t)$ deduced under the consideration of zero and non-zero axial pressure gradients.

First of all, we consider $\delta(t)$ given by Eq. (5.18) for inviscid flows and $A(t)$ given by Eq. (5.10) for zero pressure gradient.

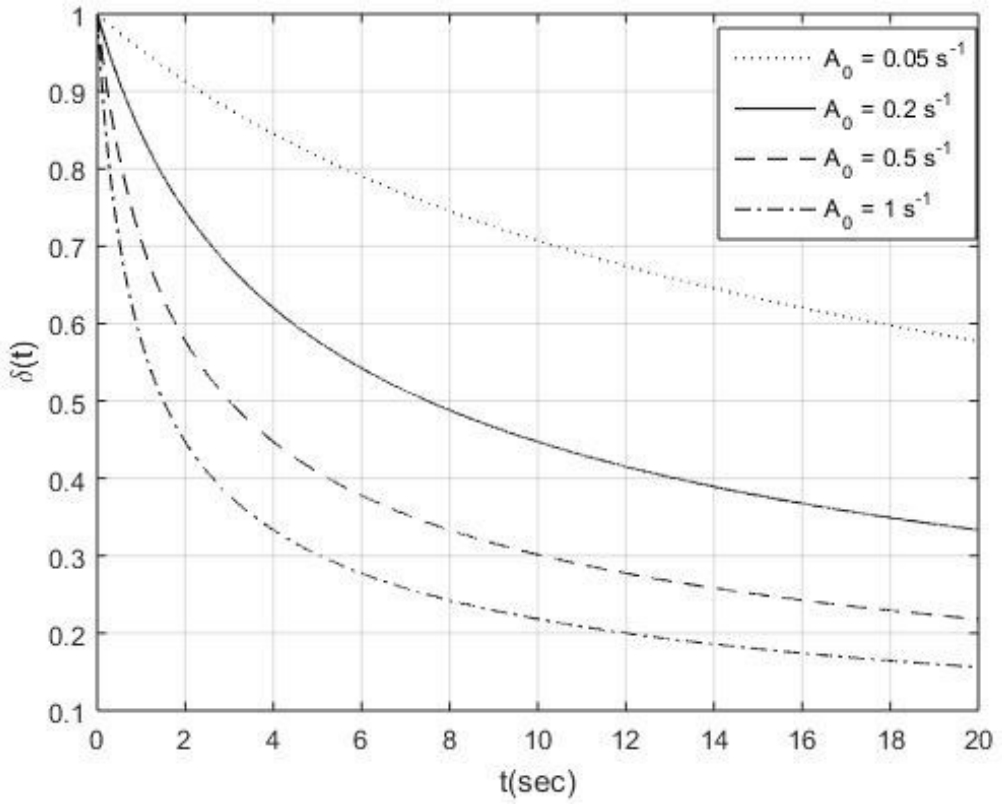

Figure 5.1: The diagram is based on Eq. (5.18) and represents the variation of core radius of vortex with time with different values of the radial flow parameter A_0 for the inviscid flow and zero axial pressure gradient. Here initial core radius $\delta(t_0) = 1\ m$.

Fig. 5.1 is plotted to display temporal variation of the core radius $\delta(t)$ as t is varied from $0 - 20\ s$, while the core radius $\delta(t_0)$ is supposed to be of $1.0\ m$ in the beginning and $A_0 = 0.05\ s^{-1}$. It is observed that the core radius $\delta(t)$ decreases initially at a fast rate but gradually slows down. We observe that in Eq. (5.18), $\delta(t) \to 0$ when $t \to \infty$. Thus, the core radius narrows with the passage of time and finally vanishes asymptotically

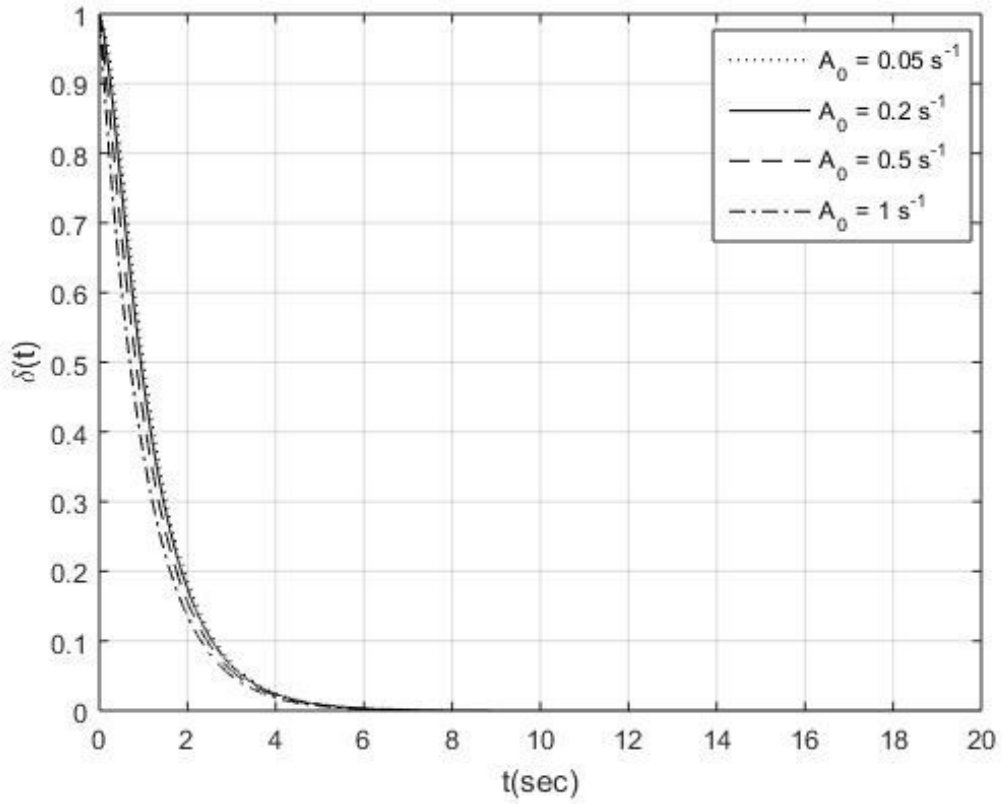

Figure 5.2: The diagram is based on Eq. (5.20) and represents the variation of core radius of vortex with time with different values of the radial flow parameter A_0 for the inviscid flow and non-zero axial pressure gradient. Here initial core radius $\delta(t_0) = 1\ m$.

Fig. 5.2 displays temporal variation of the core radius $\delta(t)$ given by Eq. (5.20) for non-zero axial pressure gradient. The range of t is maintained as the same, i.e., from $0-20\ s$ and the core radius $\delta(t_0)$ too is the same as $1.0\ m$ in the beginning with $A_0 = 0.05\ s^{-1}$. The observation is that the core radius $\delta(t)$ decreases initially at a faster rate than the previous case and slows down earlier than the previous case. Change in A_0 is not that effective; for smaller values of A_0, the core radius remains almost the same. Here too, from Eq. (5.20) we get $\delta(t) \to 0$ as $t \to \infty$, i.e., the core radius narrows with time and finally disappears. When we compare with case that pressure gradient is zero, we find that in this case $\delta(t)$ dies out very fast.

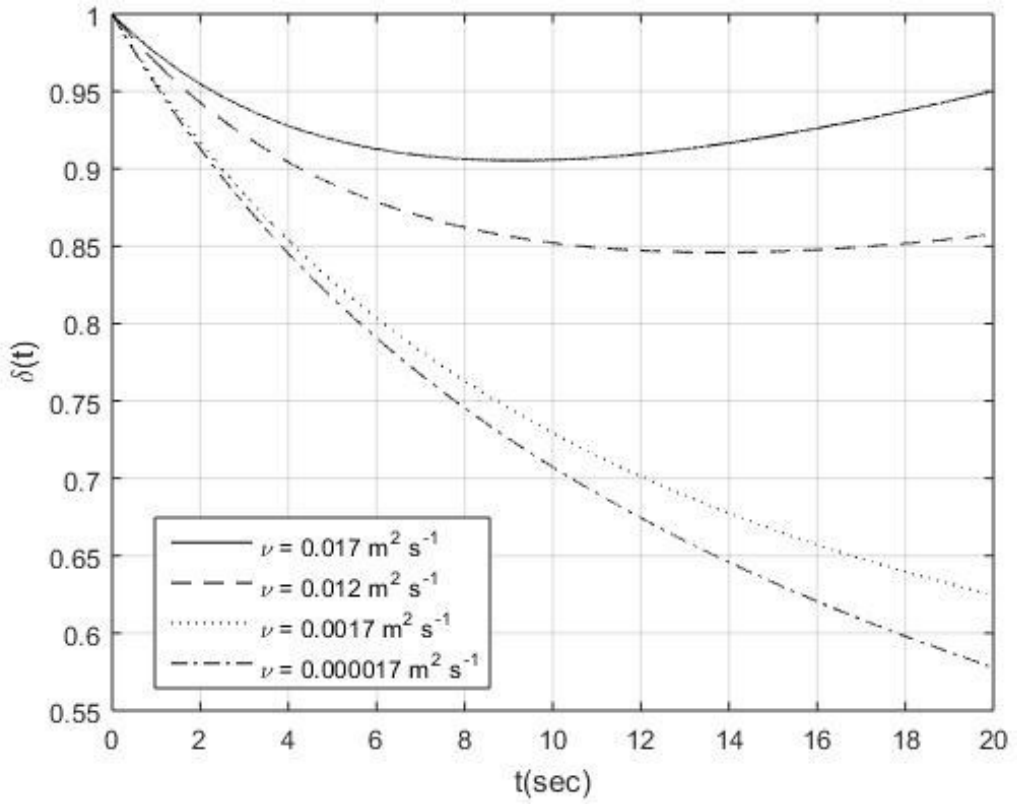

Figure 5.3: Diagram is based on Eq. (5.26) represents the variation of core radius of vortex with time for different kinematic viscosities and zero axial pressure gradient. Here, initial core radius $\delta(t_0) = 1\ m$.

The next case considered is that the flow is viscous with $\delta(t)$ given by Eq. (5.26) for zero pressure gradient. Fig. 5.3 has been plotted to discuss this case. Once again the range of t is maintained as the same, i.e., from $0-20\ s$ and the core radius $\delta(t_0)$ too is the same as 1.0 m in the beginning with $A_0 = 0.05\ s^{-1}$. The curves corresponding to $\delta(t)$ vs. t are dissimilar to those corresponding to non-viscous case (cf. Fig. 5.1 in the sense that the core radius diminishes continuously for very small kinematic viscosity but for comparatively high viscosity, it reduces first and then increases with time. This is due to the two terms of Eq. (5.26). The second term contains viscosity and makes core radius infinitely large, since $\delta(t) \to \infty$ as $t \to \infty$ in Eq. (5.26). For very small viscosity, the core radius reduces to zero as if it were

inviscid case formulated in Eq. (5.18). There may be a critical value of the kinematic viscosity for which the core radius becomes constant after some time. For somewhat larger viscosity, the core radius may increase from the beginning overcoming the non-viscous term of Eq. (5.26).

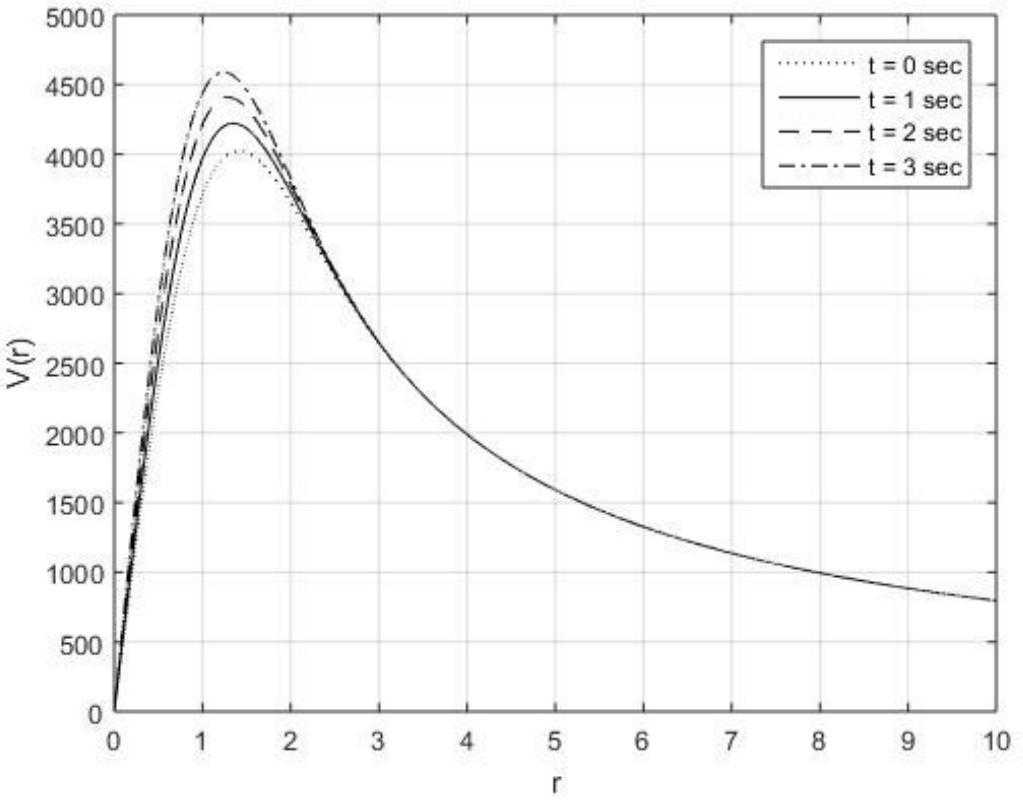

Figure 5.4: The diagram is based on Eq. (5.29) and represents the temporal variation of azimuthal velocity with radius for viscous flow and zero axial pressure gradient.

We use then the core radius to determine the azimuthal velocity. We draw plots Fig. 4 for azimuthal velocity vs. radius based on Eq. (5.29) with $M(\zeta_0) = 0$, where $\zeta_0 = r_0^2/\delta^2(t_0)$. It is observed that the azimuthal velocity rises very sharp with the radius, soon reaches the maximum at the core radius, but then gradually diminishes in magnitude at a fast rate and finally dies out satisfying equation.

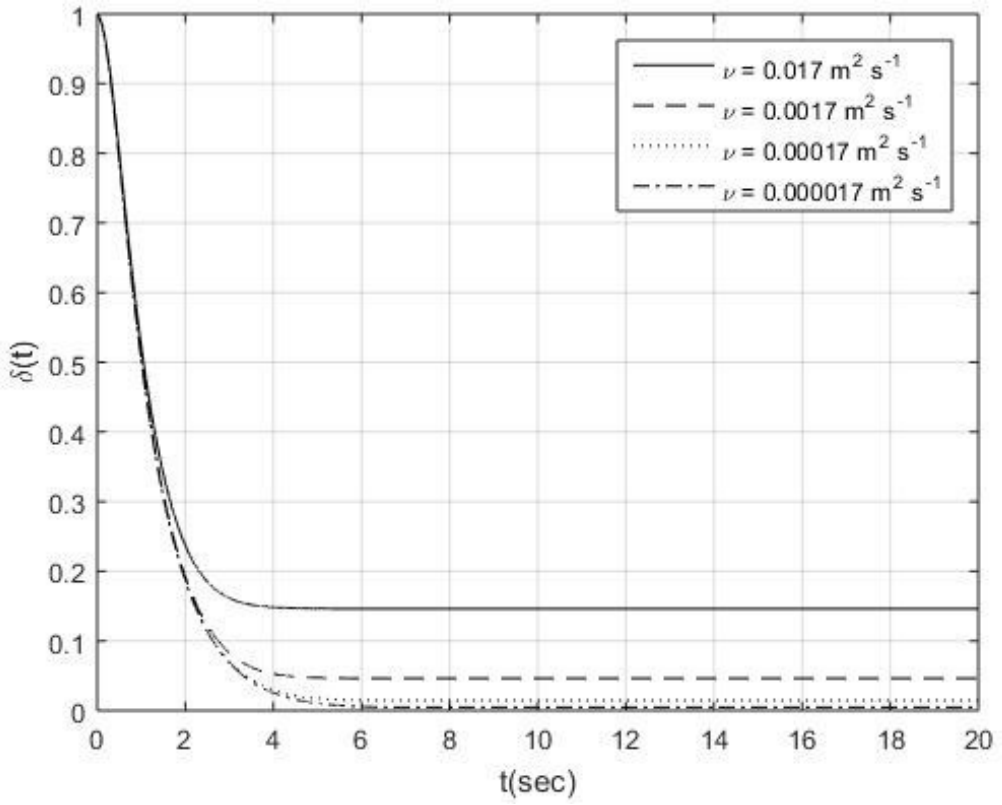

Figure 5.5: The diagram based on Eq. (5.27) represents the variation of core radius of vortex with time with different radial flow parameter A_0 for the viscous flow and non-zero axial pressure gradient. Here initial core radius $\delta(t_0) = 1\ m$ and $a = 1\ s^{-1}$.

For non-zero axial pressure gradient and viscous flows, the core radius is given by Eq. (5.27). The relation between $\delta(t)$ and t has been displayed in Fig. 5.5. It is observed that the core radius diminishes very fast with time but soon stabilises. Larger the kinematic viscosity, thicker is the core radius. In the limiting case, the similar is the observation which reveals analytically that $\delta(t) \to \sqrt{\nu C/a}$ as $t \to \infty$ (provided $a \neq 0$) from Eq. (5.27). In case $a \to 0$, $\delta(t) \to \infty$ which is similar to the conclusion made for zero pressure gradient.

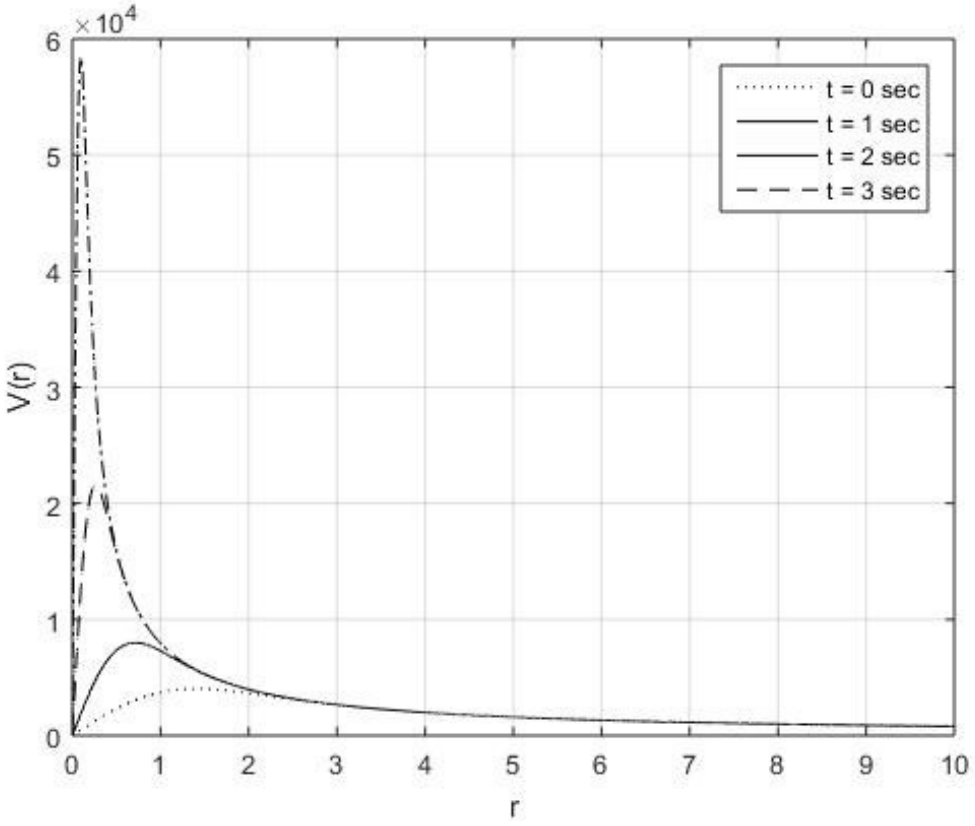

Figure 5.6: The diagram is based on Eq. (5.29) and represents the temporal variation of azimuthal velocity with radius with different time for the viscous flow and non-zero axial pressure gradient. Here kinematic viscosity $\nu = 0.000017\ m^2\ s^{-1}$ and $a = 1\ s^{-1}$.

The core radius is used to determine the azimuthal velocity. We draw plots Fig. 5.6 for azimuthal velocity vs. radius based on Eq. (5.29) with $M(\zeta_0) = 0$, where $\zeta_0 = r_0^2/\delta^2(t_0)$. The observation is similar and the azimuthal velocity rises very sharp with radius, soon reaches the maximum at the core radius, then gradually diminishes in magnitude at a fast rate and finally dies out satisfying Eq. (5.29). The magnitude of velocity is several times more than the previous case.

We further examine the dependence of maximum velocity on the core radius. The cases of inviscid and viscous flows are considered separately.

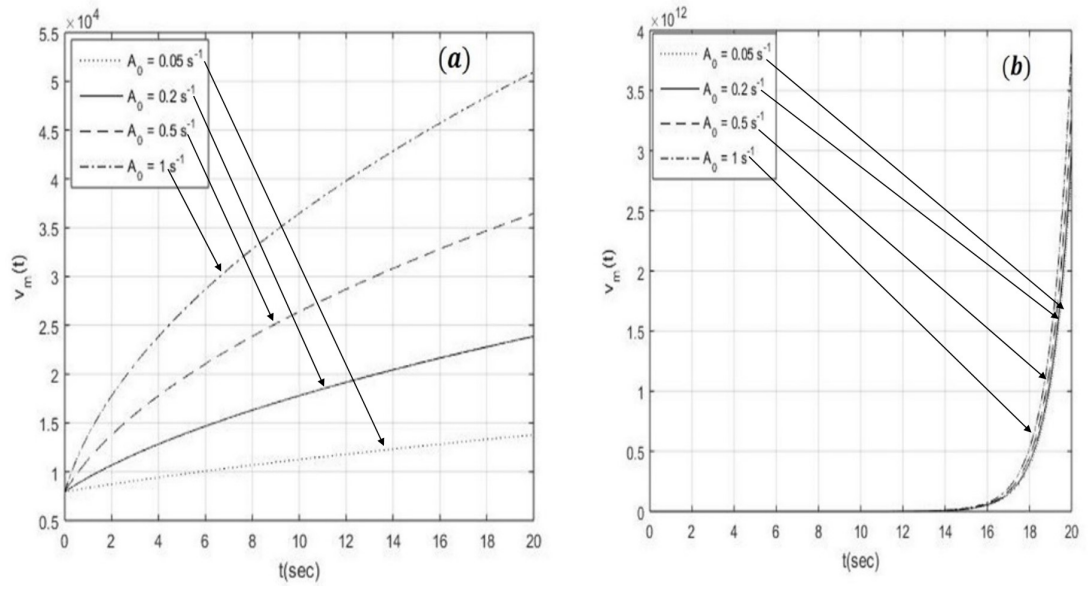

Figure 5.7: Diagram (a) based on Eq. (5.15) represents the variation of maximum azimuthal velocity vs. time for different values of radial flow parameter A_0 when the flow is inviscid and the axial pressure gradient is zero while Diagram (b) is based on Eq. (5.15) and represents variation of the maximum azimuthal velocity with time for different values of radial flow parameter A_0 when the flow is inviscid and the axial pressure gradient is non-zero.

The maximum azimuthal velocity is given by Eq. (5.15) for inviscid vortex and by Eq. (5.33) for viscous vortex. For inviscid flow, the maximum azimuthal velocity $v_m(t) = M_\infty/\delta(t)$. For $r_0 = 0$, we have $M(\zeta_0) = 0$ and $C = 2.5128$. With these values the maximum velocity for viscous flows is given by $v_m(t) = 0.71532 \times M_\infty/\delta(t)$. Thus, in both the cases $v_m(t)$ is inversely proportional to $\delta(t)$. For the various cases, $v_m(t)$ vs. t graphs are shown by Fig. 5.7 and Fig. 5.8. For constant radial flow parameter A, these formulas reduce to those presented by Davies-Jones and Wood (2006), and hence these graphs also match the patterns of experimental observation by Davies-Jones and Wood (2006) although unlike their formulations of time independent core radius, $\delta(t)$ is time dependent in our formulations, whose dependence on time has been presented in Figs. 5.1−5.6.

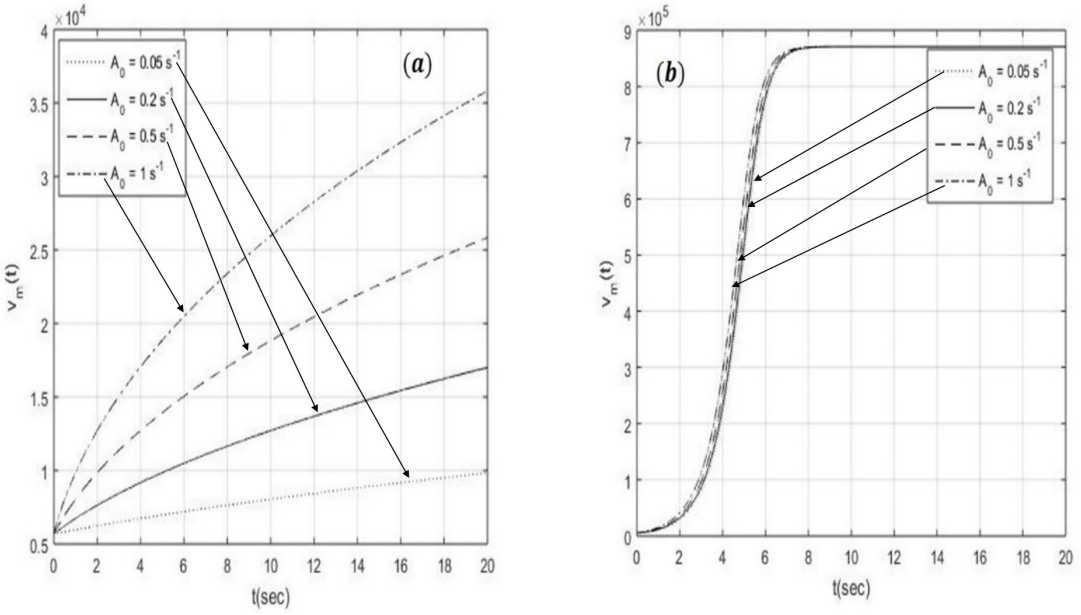

Figure 5.8: Diagram (a) based on Eq. (5.33) represents the variation of maximum azimuthal velocity vs. time for different values of radial flow parameter A_0 when the flow is viscous and the axial pressure gradient is zero while Diagram (b) is based on Eq. (5.33) and represents variation of the maximum azimuthal velocity with time for different values of radial flow parameter A_0 when the flow is viscous and the axial pressure gradient is non-zero. Here kinematic viscosity $\nu = 0.000017\ m^2\ s^{-1}$ and $a = 1\ s^{-1}$.

5.4 Conclusions

Generalised solutions to several exiting special solutions have been attempted in this paper (although more generalisations are still possible). With the assumption that $B(t) = 0$, $A(t)$ has been deduced for two cases, i.e., (1) the axial pressure gradient is zero, (2) the axial pressure gradient pressure is non-zero. Core radius is then determined for the two cases, i.e., inviscid flow and viscous flow. The azimuthal velocity is dependent on the core radius; hence we have two forms of azimuthal velocity each for inviscid and viscous flow.

Azimuthal velocity has been derived for unsteady cases, which reduces to steady forms derived by different researchers during several decades under different considerations.

In the first case with zero axial pressure gradient, it is observed that the core radius increases infinitely for viscous flow when $t \to \infty$; while for non-viscous flows, the core radius reduced to zero when $t \to \infty$, In the second case with non-zero pressure gradient we observed during discussion that the core radius becomes constant when $t \to \infty$, if the flow is viscous but vanishes for inviscid flows. With zero axial pressure gradient, i.e., $a \to 0$ the conclusion confirms the inference made in the previous case.

In both the cases, azimuthal velocity rises very sharp with the radius, soon reaches the maximum at the core radius, but then gradually diminishes in magnitude at a fast rate and finally dies out. In the second case, azimuthal velocity is found to be much larger. Further, in both the cases, the maximum azimuthal velocity $v_m(t)$ is inversely proportional to the core radius $\delta(t)$.

****